J|A|C|S
ARTICLES
Published on Web 06/07/2006

Size- and Shape-Dependent Transformation of Nanosized Titanate into Analogous Anatase Titania Nanostructures

Yuanbing Mao[†] and Stanislaus S. Wong*[,†,‡]

Contribution from the Department of Chemistry, State University of New York at Stony Brook, Stony Brook, New York 11794-3400, and Materials and Chemical Sciences Department, Brookhaven National Laboratory, Building 480, Upton, New York 11973

Received February 9, 2006; E-mail: sswong@notes.cc.sunysb.edu; sswong@bnl.gov

Abstract: A size- and shape-dependent morphological transformation was demonstrated during the hydrothermal soft chemical transformation, in neutral solution, of titanate nanostructures into their anatase titania counterparts. Specifically, lepidocrocite hydrogen titanate nanotubes with diameters of ~10 nm were transformed into anatase nanoparticles with an average size of 12 nm. Lepidocrocite hydrogen titanate nanowires with relatively small diameters (average diameter range of ≤ 200 nm) were converted into single-crystalline anatase nanowires with relatively smooth surfaces. Larger diameter (>200 nm) titanate wires were transformed into analogous anatase submicron wire motifs, resembling clusters of adjoining anatase nanocrystals with perfectly parallel, oriented fringes. Our results indicate that as-synthesized TiO_2 nanostructures possessed higher photocatalytic activity than the commercial titania precursors from whence they were derived.

Introduction

Nanoscale synthesis has traditionally relied on generating nanomaterials from bulk precursors using a number of excellent though imperfect approaches. For instance, various "top-down" strategies, such as milling, imprinting, or etching techniques, are limited with respect to the available geometries, shapes, and sizes of synthesizable nanomaterials that can be efficiently generated.[1,2] In addition, diverse "bottom-up" methodologies starting from either atomic or molecular precursors in the gaseous or solution phase often are unable to yield simultaneous control over nanoparticle structure, surface chemistry, monodispersity, crystal structure, and assembly.[3,4]

It would be conceptually easier to control the chemical structure of matter at the nanometer scale if one were able to start with, transform, and subsequently manipulate nanoscale precursors to obtain the desired target materials. One exciting strategic approach aimed at fulfilling this objective is associated with the use of localized solid-state chemical transformations via the insertion,[5,6] exchange,[3,7] or deletion[8−10] of individual atoms. In other words, existing nanostructures serve as structural templates from which nanomaterials of a diverse nature and a complex composition, which may be difficult or otherwise impossible to synthesize, can be readily generated. Collectively, these types of reactions with minor alterations could be used to produce many technologically important, nanometer-scale crystalline materials, with a wide range of size- and shape-tunable properties.[3,5−9,11] The main point involved is that classes of new nanomaterials can be created through reasonably straightforward in situ localized structural transformations, which are often modifications of versatile bulk reactions.

As a model system to demonstrate this idea, nanocrystallites of TiO_2 (titania) are of great interest for photocatalysts, gas sensors, pigments, and photovoltaic applications, because of their electronic, optoelectronic, and catalytic properties, which are intrinsically coupled to their high surface area, porosity, low cost, and chemical stability.[12] Hence, it is not surprising that groups have been highly motivated to synthesize titania nanostructures by solution chemistry methods, involving either titanium sulfates, titanium tetrahalides, titanium alkoxides, or other organometallic titanium derivatives, under various experimental conditions, such as the presence of either acidic and alkaline media.[12,13]

However, there is limited precedence for producing titania nanostructures from an existing nanoscale motif. For instance, TiO_2(B) nanowires have been prepared by heating acid-washed titanate nanowires at 400 °C for 4 h in air; the titanates in that case were initially generated by adding anatase TiO_2 to a highly

[†] State University of New York at Stony Brook.
[‡] Brookhaven National Laboratory.

(1) Mirkin, C. A.; Rogers, J. A. *MRS Bull.* **2001**, *26*, 506.
(2) Xia, Y.; Yang, P.; Sun, Y.; Wu, Y.; Mayers, B.; Gates, B.; Yin, Y.; Kim, F.; Yan, H. *Adv. Mater.* **2003**, *15*, 353.
(3) Dloczik, L.; Könenkamp, R. *Nano Lett.* **2003**, *3*, 651.
(4) Patzke, G. R.; Krumeich, F.; Nesper, R. *Angew. Chem., Int. Ed.* **2002**, *41*, 2446.
(5) Cao, M.; Wang, Y.; Qi, Y.; Guo, C.; Hu, C. *J. Solid State Chem.* **2004**, *177*, 2205.
(6) Gates, B.; Wu, Y.; Yin, Y.; Yang, P.; Xia, Y. *J. Am. Chem. Soc.* **2001**, *123*, 11500.
(7) Son, D. H.; Hughes, S. M.; Yin, Y.; Alivisatos, A. P. *Science* **2004**, *306*, 1009.
(8) Armstrong, A. R.; Armstrong, G.; Canales, J.; Bruce, P. G. *Angew. Chem., Int. Ed.* **2004**, *43*, 2286.
(9) Zhu, H. Y.; Lan, Y.; Gao, X. P.; Ringer, S. P.; Zheng, Z. F.; Song, D. Y.; Zhao, J. C. *J. Am. Chem. Soc.* **2005**, *127*, 6730.
(10) Mao, Y.; Kanungo, M.; Hemraj-Benny, T.; Wong, S. S. *J. Phys. Chem. B* **2006**, *110*, 702.
(11) Burda, C.; Chen, X.; Narayanan, R.; El-Sayed, M. A. *Chem. Rev.* **2005**, *105*, 1025.
(12) Hoffmann, M. R.; Martin, S. T.; Choi, W.; Bahnemann, D. W. *Chem. Rev.* **1995**, *95*, 69.
(13) a) Li, G.; Li, L.; Boerio-Goates, J.; Woodfield, B. F. *J. Am. Chem. Soc.* **2005**, *127*, 8659. (b) Zhang, H.; Finnegan, M.; Banfield, J. F. *Nano Lett.* **2001**, *1*, 81.

concentrated aqueous NaOH solution.[8] These TiO_2(B) nanowires could be further transformed into their anatase one-dimensional (1-D) analogues as well as into rod-shaped rutile grains between 600 to 800 °C and at 900 °C, respectively.[14] Platelike $BaTiO_3$ and anatase particles can be synthesized from an H^+-form of titanate (e.g., $H_{1.07}Ti_{1.73}O_4 \cdot nH_2O$) with a lepidocrocite-like layered structure using a hydrothermal soft chemical synthetic process.[15] Moreover, titanate nanostructures can be converted into their anatase and rutile TiO_2 nanoparticle polymorphs in simple wet-chemical conditions in acidic aqueous dispersions.[9] Very recently, we have demonstrated that as-formed, sea-urchin-like assemblies of alkali metal hydrogen titanate 1-D nanostructures could be subsequently transformed into their analogous anatase TiO_2 1-D counterparts by annealing hydrogen titanate 1-D nanostructure intermediates in air.[10]

It is noteworthy that none of these prior experiments aim to rationally dictate the size and shape of the resultant nanoscale product along the lines of a recently reported study from the Alivisatos group in selenide nanocrystal systems,[7] wherein careful analysis of the intrinsic thermodynamics, kinetics, and mechanism of nanocrystal reactions was used to obtain insights into the size ranges of nanocrystals that could be chemically transformed without loss of original shape. The gist of that work was that nanocrystal chemical reactions could undergo homogeneous, molecule-like kinetics, resembling molecular transformations, as opposed to the more complex, heterogeneous, statistically averaged kinetics characteristic of many bulk solid-state reactions.[7,11]

In the current manuscript, in the spirit of this idea, we studied the size dependence of a number of hydrothermally prepared titanate nanostructure "reagents"[16,17] in controllably preparing anatase TiO_2 products by a reasonably mild hydrothermal process coupled with a dehydration reaction.[15] In our experiments, we have been able to convert titanate nanowires and nanotubes into anatase titania nanowires and nanoparticles, respectively, at essentially 100% yield under neutral aqueous, relatively low-temperature conditions, unlike the acidic aqueous conditions used by Zhu et al.[9] In fact, we show that the size and shape of the precursor titanate structural motif strongly dictate and control the eventual morphology of the resulting titania products. This work serves as the first report of a similar localized size- and shape-dependent transformation between oxide nanostructure motifs, analogous to what has been previously observed in selenide systems.[7] Moreover, our as-synthesized crystalline anatase TiO_2 products are chemically pure, prepared without the use of either mineralizers or anionic additives.

Experimental Section

Materials Preparation. A. Titanates. In our experiments, the hydrothermal method initially developed by Kasuga et al. was employed for the synthesis of titanate nanostructures, which involved a primary reaction between a concentrated NaOH solution and titanium dioxide.[16,17] Specifically, a commercial anatase TiO_2 powder (Alfa Aesar, 0.1−1 g) was dispersed in an 18 mL aqueous solution of NaOH (5−10 M) and placed into a Teflon-lined autoclave with an 80% filling factor. The autoclave was then oven-heated at 110−190 °C for 12 h to 1 week. A white precipitate was isolated upon filtration and washed repeatedly with copious amounts (100 to 200 mL) of distilled, deionized water until the pH value of the supernatant had attained a reading close to 7. After collection by centrifugation and oven drying at 120 °C overnight, the as-produced 1-D sodium hydrogen titanate nanomaterials were neutralized using a 0.1 M HCl solution and subsequently washed with distilled, deionized water (∼100 to 200 mL until the pH of the supernatant had attained a value of ∼7) to prepare their hydrogen titanate analogues, which were subsequently oven-dried at 120 °C overnight.

B. Titania. To synthesize the corresponding anatase nanostructures, dried hydrogen titanate nanostructures (∼50 mg) were dispersed into 16 mL of distilled water for 1 h by stirring and then transferred to a 23 mL autoclave, which was kept at 170 °C in this case, for 12−36 h.[15] A white precipitate was eventually recovered upon centrifugation.

Materials Characterization. All products and intermediate precursors in this reaction, including hydrogen titanate nanostructures, were characterized by a number of different methodologies, including X-ray diffraction (XRD), Raman spectroscopy, ultraviolet−visible (UV−vis) spectroscopy, scanning electron microscopy (SEM), transmission electron microscopy (TEM), high-resolution transmission electron microscopy (HRTEM), selected area electron diffraction (SAED), and energy-dispersive X-ray spectroscopy (EDS).

X-ray Diffraction. Crystallographic and purity information on hydrogen titanate and anatase TiO_2 nanostructures were obtained using powder XRD. To analyze these materials, as-prepared samples of hydrogen titanate and anatase TiO_2, after centrifugation, were subsequently sonicated for about 1 min and later air-dried upon deposition onto glass slides. Diffraction patterns of these materials were collected using a Scintag diffractometer, operating in the Bragg configuration using Cu Kα radiation ($\lambda = 1.54$ Å) from 5° to 80° at scanning rates of 0.2° per min.

Raman Spectroscopy. Spectra were acquired with a Raman microspectrometer (Renishaw 1000) using an Ar^+ laser (514.5 nm). A 50× objective and low laser power density were chosen for irradiation of bulk hydrogen titanate and commercial anatase TiO_2 samples in addition to all of the nanostructure samples, as well as for signal collection. The laser power was kept low enough to avoid heating of the samples by optical filtering and/or defocusing the laser beam at the sample surface. Spectra were collected in the range of 1000−50 cm^{-1} with a resolution of 1 cm^{-1}.

UV−visible Spectroscopy. UV−visible spectra were obtained at high resolution on a Thermospectronics UV1 spectrometer using quartz cells with a 10-mm path length. Spectra were obtained for hydrogen titanate and anatase nanostructures which had been sonicated in distilled water to yield homogeneous dispersions. UV−visible absorption spectra were recorded using distilled water as a blank.

Electron Microscopy. The size, morphology, and chemical composition of solid powder samples of precursor hydrogen titanate and resulting anatase TiO_2 nanostructures were initially characterized using a field emission SEM (Leo FE-SEM 1550 with EDS capabilities) at accelerating voltages of 15 kV. Specifically, powders of hydrogen titanate and anatase TiO_2 nanostructures were mounted onto conductive carbon tapes, which were then attached onto the surfaces of SEM brass stubs. These samples were then conductively coated with gold by sputtering for 20 s to minimize charging effects under SEM imaging conditions.

Low magnification TEM images were taken at an accelerating voltage of 120 kV on a Philips CM12 instrument, equipped with EDS capabilities. HRTEM images and SAED patterns as well as EDS data were obtained on a JEOL 2010F HRTEM (equipped with an Oxford INCA EDS system as well as with the potential of performing SAED) at an accelerating voltage of 200 kV to further characterize the morphologies of individual nanostructures of hydrogen titanate and

(14) Yoshida, R.; Suzuki, Y.; Yoshikawa, S. *J. Solid State Chem.* **2005**, *178*, 2179.
(15) Feng, Q.; Hirasawa, M.; Yanagisawa, K. *Chem. Mater.* **2001**, *13*, 290.
(16) Bavykin, D. V.; Parmon, V. N.; Lapkin, A. A.; Walsh, F. C. *J. Mater. Chem.* **2004**, *14*, 3370.
(17) Kasuga, T.; Hiramatsu, M.; Hoson, A.; Sekino, T.; Niihara, K. *Adv. Mater.* **1999**, *11*, 1307.

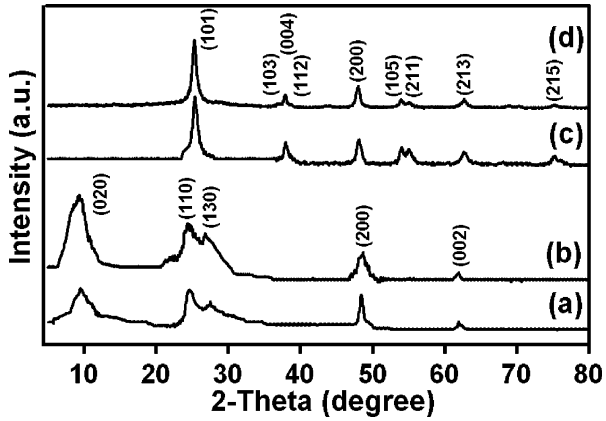

Figure 1. XRD patterns from (a) hydrogen titanate nanotubes, (b) hydrogen titanate nanowires, (c) anatase TiO_2 nanoparticles, and (d) anatase TiO_2 nanowires, respectively.

anatase TiO_2. Specimens for the TEM studies were prepared by depositing a drop of these aqueous suspension samples onto a 300 mesh Cu grid, coated with a lacey carbon film. Prior to deposition, solutions containing samples of hydrogen titanate and anatase nanostructures were sonicated for 2 min to ensure adequate dispersion in solution.

Elemental Analysis. Inductively coupled plasma mass spectroscopy (ICP-MS) was accomplished using a Perkin-Elmer Sciex Elan 6100 ICP-MS instrument. A 60-element semiquantitative metals screen was performed on representative samples. The presence of Bi was attributed to impurities originating from the autoclave.

Photocatalytic Activity. To test the photochemical efficiency of as-prepared TiO_2 samples, a solution mixture of 100 mg/L Procion Red MX-5B (Aldrich) containing 100 mg/L TiO_2 nanostructures in water was prepared under irradiation with a UV lamp (maximum emission wavelength at 365 nm) at a ~5 cm separation distance. Analogous control experiments were performed either without TiO_2 (blank) or with commerical nanosized TiO_2. At given irradiation time intervals, 10 mL aliquots were sampled and centrifuged to remove remnant TiO_2 particles. Supernatant aliquots were subsequently analyzed by UV−visible spectroscopy at high resolution using a Thermospectronics UV1 spectrometer with 10-mm path length quartz cells.

Results and Discussion

The main gist of our data is that we were able to controllably prepare hydrogen titanates of varied sizes and shapes, obtained at different reaction temperatures.[16] Upon subsequent reaction, these nanoscale precursors yielded nanosized titania products whose structural morphology was intrinsically dependent on the size and shape of the starting reagent nanomaterial. We summarize our results as follows and thereafter systematically describe our experimental results in detail.

(i) Hydrogen titanate nanotubes (~7 to 10 nm in diameter) were transformed into single-crystalline anatase nanoparticles.

(ii) Small-diameter hydrogen titanate nanowires (≤200 nm) were converted into single-crystalline anatase nanowires with relatively smooth surfaces.

(iii) Large-diameter hydrogen titanate wires (~200 to 500 nm) were altered into anatase wires, resembling clusters of adjoining anatase nanocrystals with perfectly parallel, oriented fringes.

XRD. As-prepared solid samples of both hydrogen titanate and anatase nanostructures were examined by powder XRD measurements (Figure 1). The XRD patterns of both hydrogen titanate nanotubes and nanowires (Figure 1a and b, respectively) do not correspond to either pristine titania phases of anatase, rutile, or brookite, or to a mixture thereof. In fact, based on the

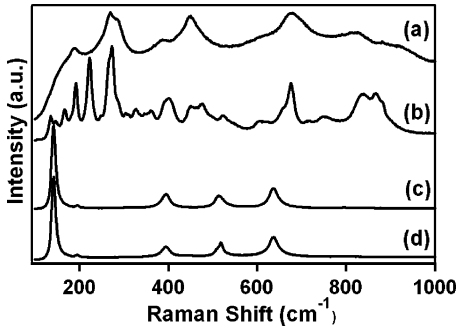

Figure 2. Raman spectra of (a) as-prepared hydrogen titanate nanowires, (b) bulk $H_2Ti_3O_7$, (c) as-prepared anatase TiO_2 nanowires, and (d) commercially available 5 nm anatase nanoparticles, respectively.

experimental data, it is more appropriate to ascribe the crystal structure of our as-prepared hydrogen titanate nanotubes and nanowires to that of a structural variant of $H_2Ti_3O_7$. More specifically, it is reasonable to assign our XRD patterns to those of an orthorhombic protonic lepidocrocite ($H_xTi_{2-x/4}\square_{x/4}O_4$ (x ~0.7, □: vacancy)) structure because of the observation of 2θ values at 9.6°, 24.7°, 28.02°, 48.22°, and 62°, which can be attributed to the relevant 020, 110, 130, 200, and 002 peaks, respectively.[10,18,19] We have also observed an as-yet unexplained, stronger intensity of the (020) reflection for nanowires as compared with that of the corresponding nanotubes.

All of the diffraction peaks in Figure 1c and d after further hydrothermal treatment of the hydrogen titanate nanostructures prepared under neutral conditions could be indexed to the pure hexagonal anatase phase of TiO_2. The intensities and positions of the observed peaks are in good agreement with literature values (space group $I4_1/amd$; JCPDS File No. 21-1272).[13] No peaks of the rutile or brookite phase were detected, indicating satisfactory purity of the products.

Raman Spectroscopy. Since Raman spectra of both as-prepared hydrogen titanate nanowires and nanotubes were essentially identical, only the spectrum of hydrogen titanate nanowires is presented in Figure 2a, which displays very broad bands near 195, 280, 450, 680, and 920 cm^{-1}, respectively. In agreement with the XRD data previously discussed, the observed spectrum shows very similar peak positions and profiles to that of protonic lepidocrocite titanate ($H_xTi_{2-x/4}\square_{x/4}O_4$ (x ~0.7, □: vacancy)).[10,19,20] By contrast, the spectrum of a bulk $H_2Ti_3O_7$ sample, generated by the neutralization of a bulk $Na_2Ti_3O_7$ product obtained commercially (Aldrich), is presented as spectrum b in Figure 2. It is evident that with this as-prepared bulk $H_2Ti_3O_7$ sample, there is an abundance of sharp peaks in the lower wavenumber regime of 100−400 cm^{-1} as well as a characteristically strong peak near ~850 cm^{-1},[10,19] all of which are absent in the spectrum of our as-prepared 1-D hydrogen titanate nanostructures. This observation is consistent with ascribing our structures to the presence of protonic lepidocrocite titanate ($H_xTi_{2-x/4}\square_{x/4}O_4$ (x ~0.7, □: vacancy)) sheets. The sole caveat is that because there are few reports directly relating observed Raman peaks to specific active modes of layered titanates, the exact assignment of the bands in the Raman spectra may not be fully accurate.

(18) Ma, R.; Bando, Y.; Sasaki, T. *Chem. Phys. Lett.* **2003**, *380*, 577.
(19) Ma, R.; Fukuda, K.; Sasaki, T.; Osada, M.; Bando, Y. *J. Phys. Chem. B* **2005**, *109*, 6210.
(20) Sasaki, T.; Nakano, S.; Yamauchi, S.; Watanabe, M. *Chem. Mater.* **1997**, *9*, 602.

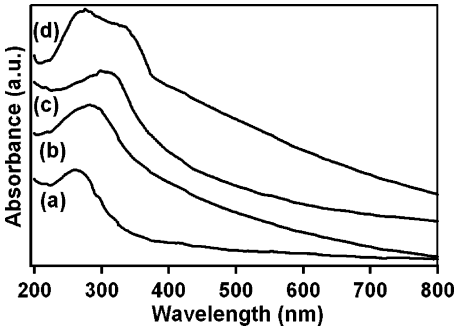

Figure 3. UV−vis spectra of as-prepared (a) hydrogen titanate nanotubes, (b) hydrogen titanate nanowires, (c) anatase TiO_2 nanoparticles, and (d) anatase TiO_2 nanowires, respectively. The curves are shifted vertically for clarity.

The Raman spectrum of TiO_2 nanostructures (Figure 2c) shows the presence of five characteristic peaks, expected of anatase. No other peaks, corresponding to other titania phases, were observed, indicating that our as-prepared titanium dioxide nanostructures were likely pure anatase in phase. In fact, observed peaks at 143 cm^{-1} (E_g), 197 cm^{-1} (E_g), 399 cm^{-1} (B_{1g}), 519 cm^{-1} (B_{2g}), and 639 cm^{-1} (E_g) matched well with those of single crystalline anatase (Figure 2c).[21] Moreover, the presence of well-resolved, higher-frequency Raman lines with substantial intensities indicated that the nanostructures were highly purified with few defects.[22] Figure 2d shows the Raman spectrum of a sample of 5 nm anatase nanoparticles, obtained commercially from Alfa Aesar as a comparison.

UV−visible Spectroscopy. UV−visible spectra of as-prepared protonic lepidocrocite titanate and titania nanostructures are shown in Figure 3. It is evident that for all the protonic lepidocrocite titanate and titania nanostructure samples, there is a broad band absorption from 250 to 350 nm, due to the transition from the O^{2-} antibonding orbital to the lowest empty orbital of Ti^{4+}.[23] Moreover, the absorption band of the smaller-sized (tens of nm) protonic titanate nanotubes (Figure 3a) is blue shifted relative to that of the relatively larger (hundreds of nm) protonic titanate nanowires (Figure 3b). This blue shift can be rationalized based on a previous study, wherein it was found that, with decreasing sample size, the optical edge tended to shift to higher energy, a phenomenon which was attributed to quantum size and confinement effects.[24] The corresponding absorption bands of anatase nanoparticles and of anatase TiO_2 nanowires are shown in Figure 3c and 3d, respectively. We also noted that the positions of the absorption peaks of protonic titanate and anatase titania samples suggest that these materials are wide band gap semiconductors, a conclusion which is consistent with previous reports.[9,12]

Microscopy of Protonic Titanate Nanostructures. A. Nanotubes. Figure 4a and 4b indicated that the titanate sample, prepared at 120 °C under hydrothermal conditions, consisted of a large quantity of nanotubes with lengths in the range of several hundred nanometers, outer diameters of ∼7−10 nm, and inner diameters of 3−5 nm. HRTEM observations revealed that

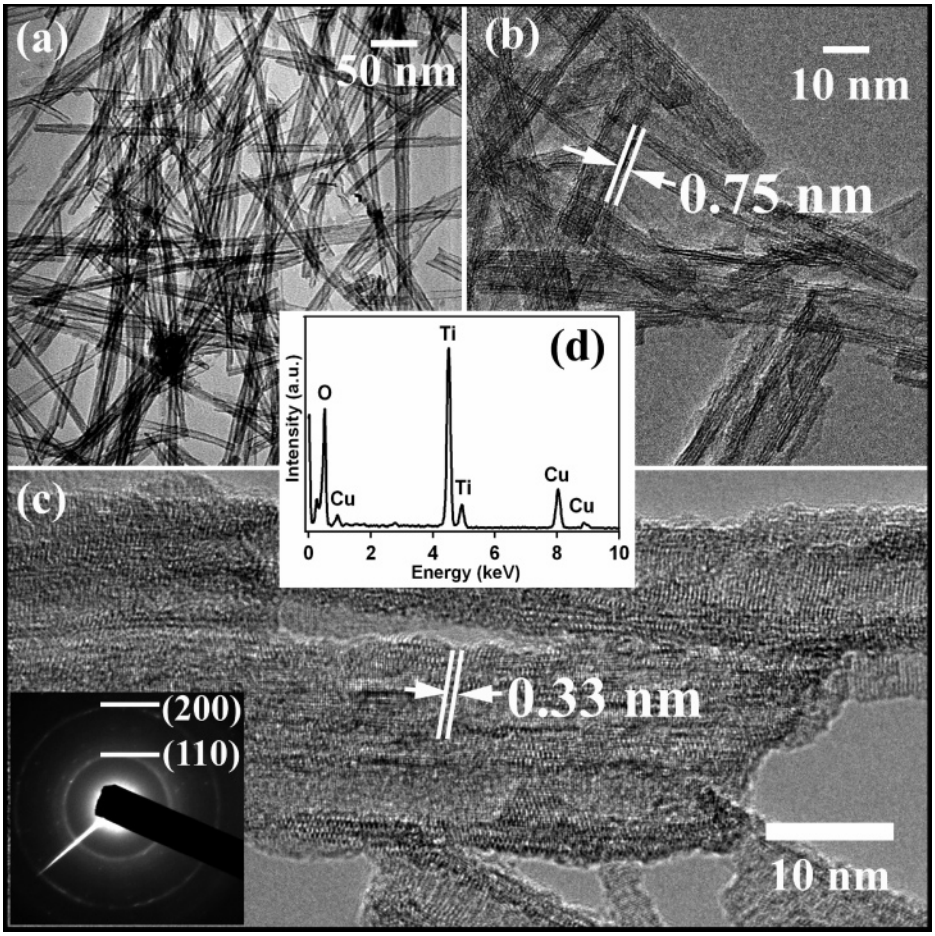

Figure 4. As-prepared hydrogen titanate nanotubes. (a) Low magnification TEM image. (b) and (c) HRTEM images. The inset of (c) shows an electron diffraction (ED) pattern. (d) EDS spectrum. The Cu peaks originate from the TEM grid.

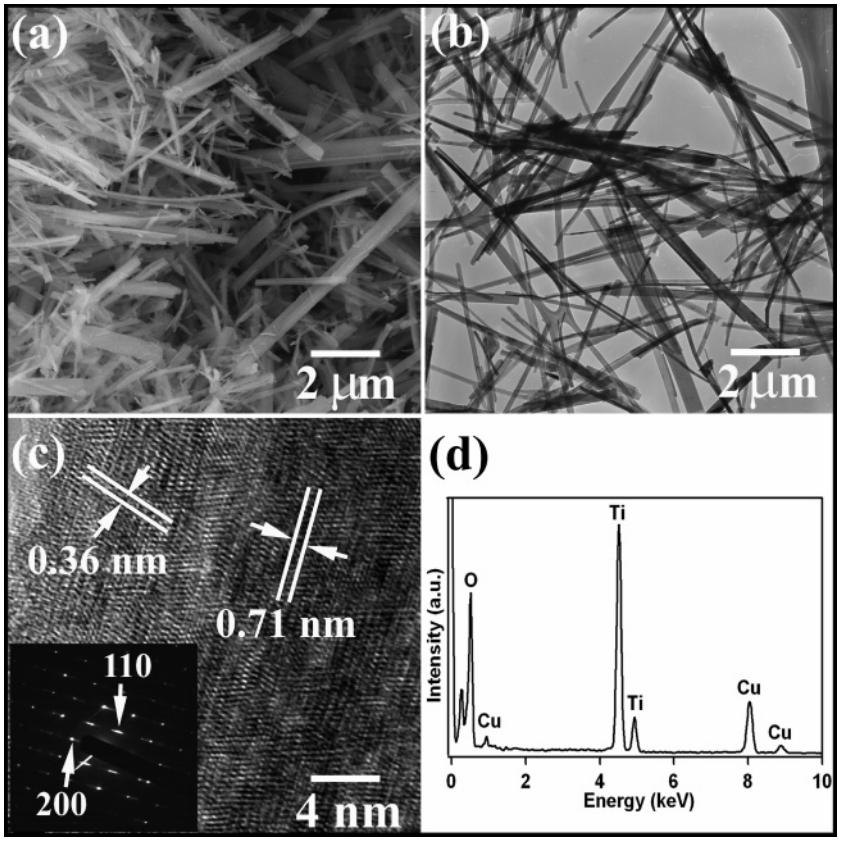

Figure 5. As-prepared hydrogen titanate nanowires. (a) Typical SEM image. (b) TEM image. (c) HRTEM image. The inset shows the corresponding SAED pattern. (d) EDS data. The Cu peaks originate from the TEM grid.

these nanotubes normally consisted of three to five layers in terms of wall thickness (Figure 4b).

The measured interlayer spacing was found to be about 7.5 Å (Figure 4b); the *d* spacing measurement perpendicular to the tube axis yielded a value of 3.3 Å (Figure 4c). It is well-known that protonic titanates can dehydrate during experimental microscopy conditions because of the high vacuum environment and the bombarding effect of electrons, which may collectively lead to a degree of shrinkage in the interlayer spacing.[18] Thus, the interlayer distances measured from the HRTEM images herein may not be as accurate and most likely decreased upon loss of hydrated water. This possibility is consistent with our observation that the perfect lattice tended to degrade after a few seconds of electron beam irradiation. We therefore considered it reasonable to index the observed 7.5 Å distance to d_{020} and the measured 3.3 Å distance to d_{110}, respectively, of an orthorhombic protonic lepidocrocite ($H_xTi_{2-x/4}\square_{x/4}O_4$ ($x \sim 0.7$, □: vacancy)) structure. In fact, the inset of Figure 4c yields an SAED pattern, with the two rings indexed to the (200) and (110) diffraction planes, respectively, of the orthorhombic lepidocrocite structure. The EDS data (Figure 4d) clearly indicate that the titanate nanotubes are composed of Ti and O, as expected. No Na was detected in the nanostructures, after washing with HCl. Taking into consideration the likely presence of H in the product, this sample can therefore be attributed to a protonic titanate species, in agreement with XRD and Raman results.

B. Nanowires. Figure 5a and 5b show representative SEM and TEM images taken from the as-synthesized protonic titanate nanowires, neutralized from sodium hydrogen titanate nanowires that had been prepared under hydrothermal conditions at 180 °C. In this sample, the as-prepared nanowires were measured to be a few microns long and ~65 to 400 nm wide. Two distinctive populations of diameter distributions of protonic titanate nanowires were observed (Figure S1). Though these nanowires tended to aggregate fairly easily, as can be observed from the SEM image (Figure 5a), sonication could readily resolve this problem, as shown in the corresponding TEM image (Figure 5b).

The HRTEM image (Figure 5c) indicates that, in this particular nanowire sample, the interlayer distance measured along the wire is ~0.71 nm, whereas the interlayer distance measured perpendicular to the wire is ~0.36 nm. Once again, considering the likelihood of sample dehydration during microscopy observations,[18] the 0.71 nm distance could be indexed to d_{020}, whereas the 0.36 nm distance could be assigned to d_{110} of $H_xTi_{2-x/4}\square_{x/4}O_4$ ($x \sim 0.7$, □: vacancy). The inset of Figure 5c yields an SAED pattern, which can be indexed to the (200) and (110) diffraction planes, respectively, of the orthorhombic lepidocrocite structure, although some displacement of the original spots was noted, indicating that a structural transformation had taken place upon electron beam exposure.[18] The EDS spectrum (Figure 5d) clearly indicates that the titanate nanowires are composed solely of Ti and O. As with the titanate nanotubes, no Na was detected in the nanostructures after washing with HCl, though the presence of Na was noted by ICP-MS (Table S1). Moreover, taking into consideration the likely presence of H in the product, this nanowire sample can therefore be attributed to a protonic titanate species, in agreement with XRD and Raman results.

Microscopy of Titania Nanostructures. A. Nanoparticles. After an additional hydrothermal cycling involving precursor

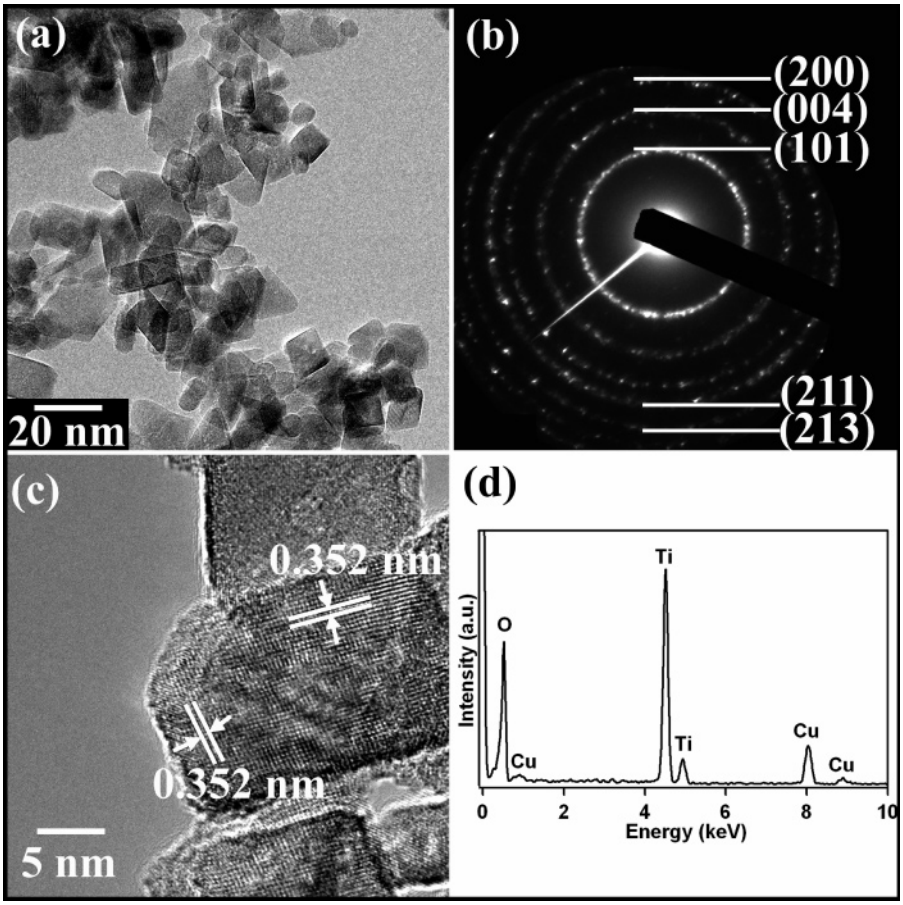

Figure 6. As-prepared anatase TiO_2 nanoparticles. (a) TEM image. (b) ED pattern. (c) HRTEM image. (d) EDS data. The Cu peaks originate from the TEM grid.

titanate nanotubes reacted at 170 °C for 24 h, all of the nanosized protonic lepidocrocite titanate nanotube precursors were transformed into corresponding anatase TiO_2 nanoparticles, which mainly consisted of nanoscale cubes and rhombohedra, as demonstrated by the TEM image in Figure 6a. These nanoparticles have an average size of 12 ± 2 nm. Figure 6b shows an SAED pattern, with the five rings indexed to the (101), (004), (200), (211), and (213) diffraction planes, respectively, of the hexagonal structure of anatase TiO_2, in agreement with that of bulk crystal data. In the HRTEM image of the resulting anatase TiO_2 nanoparticles (Figure 6c), one can clearly observe a 0.352 nm lattice spacing between the (101) planes. The EDS spectrum (Figure 6d) shows that these TiO_2 nanoparticles are elementally composed of Ti and O, with the Cu peaks originating from the TEM grid.

Based on these data, we can conclude that the TiO_2 nanoparticles synthesized using this method are single-crystalline titania, with a hexagonal structure similar to that of the bulk crystalline anatase solid. This assertion is in agreement with the XRD pattern and Raman spectrum data (Figure 1c and 2c), taken from a collection of TiO_2 nanoparticles. It is worth noting that previous methodologies aimed at synthesizing anatase nanoparticles have been primarily associated with either sol−gel methods involving the use of titanium tetrachloride or titanium alkoxide precursors or through solution chemistry techniques associated with titanium sulfates.[13a] In these prior reports, such protocols have tended to be associated with the generation of either chemical impurities or minor impurity phases in the final anatase TiO_2 products.[13b]

By contrast, our synthesis yields anatase TiO_2 nanoparticles with controllable chemical composition (without the obvious presence of impurities) as well as particle morphology, produced under hydrothermal conditions in neutral aqueous solvent without the use of mineralizers, anions, or similar additives (such as SO_4^{2-}, NH_4Cl, NaCl, $SnCl_4$, and so forth). Nonetheless, we cannot discount the possibility that there may be a significant amount of hydroxyl species on the surfaces of these nanoparticles, which would be beneficial for an enhanced photocatalytic activity of these materials.[25,26]

B. Nanowires. Anatase TiO_2 nanowires were synthesized by a similar hydrothermal soft chemical synthetic method. In this case, protonic lepidocrocite titanate nanowire precursors were used instead. As with the anatase TiO_2 nanoparticle synthesis, the reaction was also run at 170 °C for 24 h. The FESEM image (Figure 7a) and TEM image (Figure 7b) show that anatase TiO_2 nanowires are formed. We note that the surfaces of the smaller diameter ($\leq$ 200 nm) nanowires formed are uneven as compared

(21) Busca, G.; Ramis, G.; Amores, J. M. G.; Escribano, V. S.; Piaggio, P. *J. Chem. Soc., Faraday Trans.* **1994**, *90*, 3181.
(22) Zhao, Y.; Lee, U.-H.; Suh, M.; Kwon, Y.-U. *Bull. Korean Chem. Soc.* **2004**, *25*, 1341.
(23) Xu, Z.; Shang, J.; Liu, C.; Kang, C.; Guo, H.; Du, Y. *Mater. Sci. Eng. B* **1999**, *63*, 211.
(24) Brus, L. E. *J. Phys. Chem.* **1986**, *90*, 2555.
(25) Cao, L.; Huang, A.; Spiess, F.-J.; Suib, S. L. *J. Catal.* **1999**, *188*, 48.
(26) Vorontsov, A. V.; Altynnikov, A. A.; Savinov, E. N.; Kurkin, E. N. *J. Photochem. Photobiol. A* **2001**, *144*, 193.

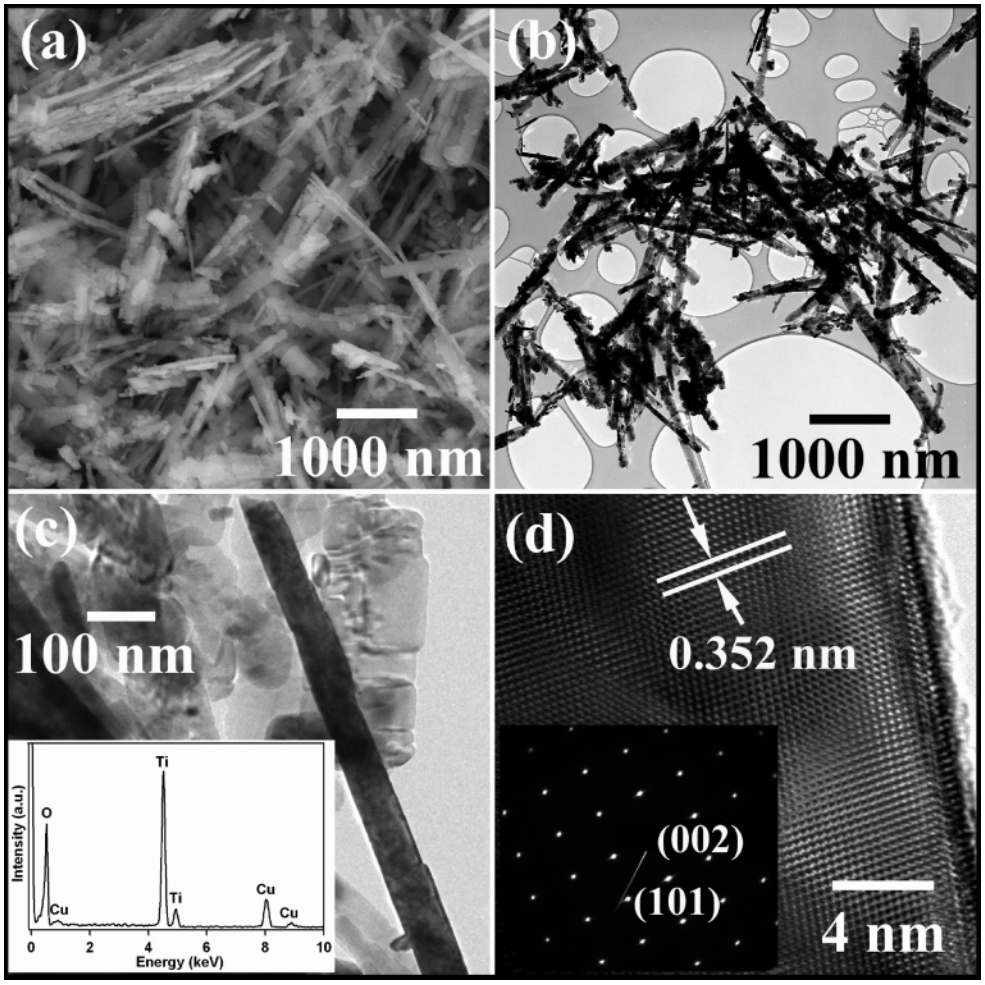

Figure 7. As-prepared anatase TiO_2 nanowires. (a) General SEM image. (b) TEM image. An individual anatase nanowire with a diameter of ~80 nm: (c) TEM image. The inset shows EDS data. The Cu peaks originate from the TEM grid. (d) HRTEM taken from a portion of the nanowire shown in (c). The inset depicts the corresponding SAED pattern.

with those of the precursor protonic titanate nanowires, while the surfaces of the larger diameter (~200 to 500 nm) wires synthesized are noticeably rougher than those of the precursor protonic titanate nanowires. In addition, clusters of some as-formed nanoparticles also were detected in this sample.

Figure 7c illustrates an individual anatase nanowire with a diameter of around 80 nm and with a length of up to a few microns. The EDS data (inset to Figure 7c) clearly show that the nanowires are composed of Ti and O elements alone; ICP-MS data further confirm the lack of any high concentrations of impurities (under 0.1%) (Table S1). In the HRTEM image (Figure 7d) taken from a portion of the individual anatase nanowire shown in Figure 7c, one can observe a 0.352 nm lattice spacing between the (101) planes, indicating that the nanowires have a [101] orientation. The inset to Figure 7d shows the SAED pattern, indexed to the (101) and (002) diffraction planes, respectively, of the hexagonal structure of anatase. Moreover, the HRTEM images and SAED patterns taken from different positions along the nanowire were found to be essentially identical within experimental accuracy, indicating that the entire nanowire is likely to be single-crystalline. We cannot necessarily negate the possibility that an amorphous coating covers the outer surfaces of some of these nanoscale structures.

Figure 8 demonstrates a few representative TEM and HRTEM images of a larger-diameter, individual anatase TiO_2 wire. Its width is around 400 nm, and its length can range up to several microns. It is evident though that this wire structure is completely covered by or otherwise composed of aggregates of discrete anatase TiO_2 nanocrystals (Figure 8a). Three representive HRTEM images (Figure 8b−d, S2−4) taken along the length of an individual, larger diameter wire shows that this wirelike structure is actually composed of a string of adjoining anatase TiO_2 nanocrystals. Strong faceting of the nanocrystal building blocks and the presence of defects at interfaces are clearly observed in these images. These as-formed nanocrystals are interconnected and aligned onto the adjoining wire surface with perfectly parallel lattice fringes, without the apparent presence of misorientations, though these cannot be fully discounted. That is, the anatase TiO_2 nanoparticles are all in the same orientation as the underlying uniaxial wire motif. The spacings of the lattice fringes were found to be about 0.352 and 0.475 nm, respectively, as further shown in Figures S2−4. These two planes could be well indexed as [101] and [002] lattice orientations of the anatase TiO_2 crystal, respectively, according to JCPDS card No. 21-1272. The measured angle between these two planes is 68.3°, matching closely with the calculated value based on JCPDS card No. 21-1272 literature data. The oriented arrangement of the anatase TiO_2 nanocrystals was confirmed by SAED analysis, which exhibited only one set of diffraction patterns along the entire wire (inset of Figure

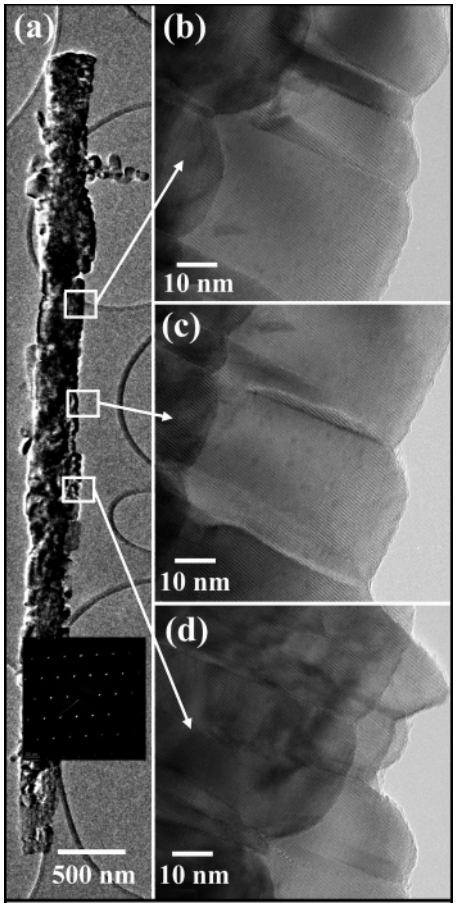

Figure 8. An individual submicron-sized anatase TiO_2 wire with a diameter of approximately 400 nm: (a) TEM image. The inset shows the corresponding SAED pattern. (b−d) HRTEM images taken from portions along the wire shown in (a), as delineated by individual white squares.

8a and Figure S5). The same SAED pattern shown in the inset of Figure 8a was enlarged in Figure S5 and indexed to [101] and [002] planes, consistent with the HRTEM results. Our data therefore suggest that anatase TiO_2 nanocrystals, constituting the wirelike aggregates, are essentially aligned in the same orientation and that, hence, our as-synthesized anatase TiO_2 wires (including both as-formed small nanowires as well as nanocrystal aggregates) grow along the [101] direction, regardless of the actual wire diameter.

Plausible Formation Mechanism. A. Protonic Lepidocrocite Titanate Nanotubes to Titania Nanoparticles. Our results suggest that the diameter, i.e., the thickness, of the precursor nanostructure may be a critical determinant factor in governing the resultant shape of the product nanomaterial.[7] It has been observed that, at the nanoscale, there are changes in the reaction free energy and the height of the reaction barrier, relative to the bulk.[27,28] For instance, by analogy to quantum dots, in the thin precursor protonic titanate nanotubes, the width of the reaction zone can become comparable in dimension to the whole width of the nanotube, due to the relatively small number of atomic layers present within a few nanometers of the structure. Hence, the slow propagation of the reaction front, driven by the gradient of the local chemical potential at or near the reaction zone, may no longer be the rate-limiting step of the reaction. Moreover, the thin protonic titanate nanotube may be in a structurally nonequilibrium state and, therefore, merely rearrange into its more stable thermodynamic state. Not surprisingly, for the thin protonic titanate nanotubes, a change of morphology to the thermodynamically more stable sphere, cube, or rhombohedron may occur, before the constituent ions have had the opportunity to diffuse, reorganize, and ultimately attain their kinetic equilibrium positions in the product.[7,29]

B. Protonic Titanate Nanowires to Anatase Titania Nanowires/Nanocrystal Aggregates. With lepidocrocite protonic titanate nanowire precursors, which are thicker than nanotubes and which appear to maintain their nonequilibrium shapes upon reaction, the reaction zone is not as affected by width considerations of the nanowire itself. Hence, propagation of the reaction front occurs, and the precursor nanostructure morphology is retained in the final titania product.[7]

The transformation of larger-diameter hydrogen titanate nanowires (in this case, between 200 and 500 nm) into structures composed of aggregates of anatase TiO_2 nanocrystals and of smaller-diameter hydrogen titanate nanowires into single-crystalline anatase TiO_2 nanowires can be explained by several plausible scenarios. For example, one group observed hydrogen titanate nanofibers covered with aggregates of anatase nanocrystals.[30] To explain this, it was proposed that the phase transition from titanate to anatase occurred through a topochemical reaction process,[30] in which the hydrogen titanate nanofibers dehydrated due to a reaction with acid, yielding anatase. It was assumed, because of the retention of the nanowire motif, that this dehydration process was accompanied by an in situ phase conversion (albeit incomplete due to formation of a composite structure), rather than through outright dissolution of titanate and atom-by-atom recrystallization of anatase.

In our study, no acid was used. However, we note that the lattice mismatch between the (110) plane of protonic lepidocrocite titanate nanowire substrate and the (101) plane of the anatase TiO_2 nanocrystals is very small (∼2%);[31a] the interplanar distances of d_{110} (3.59 Å, protonic titanate) and d_{101} (3.52 Å, anatase TiO_2) involved are rather similar. The protonic lepidocrocite titanate lattice, $H_xTi_{2-x/4}\square_{x/4}O_4$ ($x \sim 0.7$, □: vacancy), is composed of two-dimensional lepidocrocite γ-(FeOOH)-type sheets in which TiO_6 octahedra are connected to each other via edge-sharing and protons are localized between the layers. In other words, the individual lepidocrocite-type host layer resembles a continuous, planar two-dimensional array.[18,20] We have clearly observed the layered nature of our protonic titanate structures from HRTEM images of titanate tubes and wires (Figures 4b and 5c). Because these particular crystallographic features are also common to the anatase TiO_2 lattice and because these lattices are essentially perfectly aligned, it is reasonable to postulate that single-crystalline anatase TiO_2 nanocrystals can form and grow in situ from the protonic titanate nanowire surface (Figure 9).[9,31a] That is, the low interfacial lattice mismatch between titanate and titania could lower the heteronucleation energy barrier required for growth of the nanoparticles.[31b]

(27) Van Hove, M. A. *J. Phys. Chem. B* **2004**, *108*, 14265.
(28) Maradudin, A.; Melngailis, J. *Phys. Rev.* **1964**, *133*, A1188.
(29) Paritskaya, L. N.; Kaganovskii, Y.; Bogdanov, V. V. *Solid State Phenom.* **2003**, *94*, 25.
(30) Zhu, H.-Y.; Gao, X.-P.; Lan, Y.; Song, D.-Y.; Xi, Y.-X.; Zhao, J.-C. *J. Am. Chem. Soc.* **2004**, *126*, 8380.
(31) (a) Yang, H. G.; Zeng, H. C. *J. Am. Chem. Soc.* **2005**, *127*, 270. (b) Zhang, D.-F.; Sun, L.-D.; Jia, C.-J.; Yan, Z.-G.; You, L.-P.; Yan, C.-H. *J. Am Chem. Soc.* **2005**, *127*, 13492.

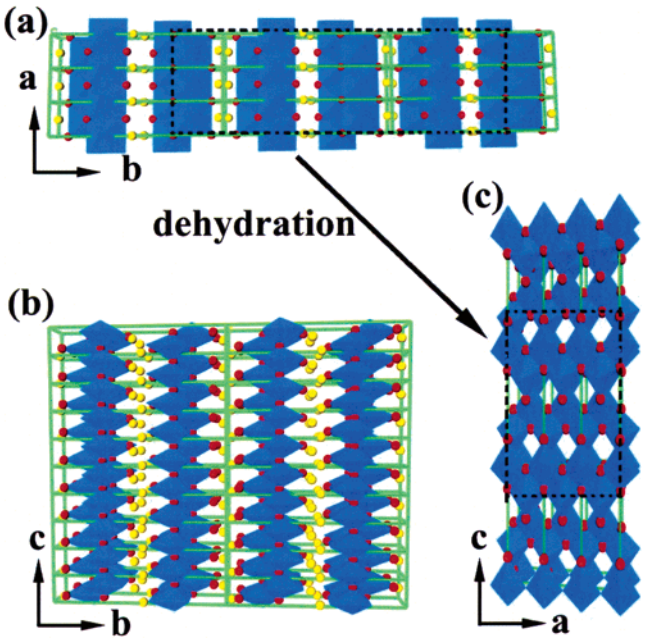

Figure 9. Schematic representations of crystal structures for the orthorhombic protonic lepidocrocite ($H_xTi_{2-x/4}\square_{x/4}O_4$ ($x \sim 0.7$, □: vacancy)) titanate structure (a and b) and its reconstruction to anatase TiO_2 (c). TiO_6 octahedra are in blue, oxygen atoms are in red, and hydrogen atoms are in yellow. (a) View along the *c*-axis showing structural features, associated with the (110) faces of titanate ($3 \times 3 \times 1$ cells). (b) View along the *a*-axis illustrating structural features corresponding to the (011) faces of titanate ($1 \times 2 \times 10$ cells). (c) View along the *b*-axis depicting structural features along the (101) faces of anatase TiO_2 ($3 \times 1 \times 3$ cells).

Hence, while the aggregation of small, independently generated anatase TiO_2 nanoparticles on the surfaces of protonic titanate nanowires is an attractive option, we believe our observations are better suited to a direct deposition process relying on an in situ nucleation event followed by subsequent oriented crystal growth and precipitation of tiny anatase TiO_2 nanoparticles onto the underlying protonic titanate backbone. That is, we hypothesize localized dissolution of the precursor protonic titanate nanowires and an in situ transformation into spontaneously oriented anatase TiO_2 nanoparticles, undergoing self-aggregation. This is the basis of the so-called "contact epitaxy" mechanism, previously observed for silver clusters supported on a Cu(001) surface.[32−34] In our case, the driving force for this spontaneous oriented attachment is the small lattice mismatch between the (110) plane of protonic titanate and (101) plane of anatase TiO_2; the elimination of this pair of high energy surfaces leads to a substantial reduction in the surface free energy of the resulting interface, thermodynamically speaking.[35,36] This effect is coupled with mechanical relaxation of the highly stressed interface upon epitaxial alignment of the anatase TiO_2 nanocrystals with the underlying protonic lepidocrocite titanate nanowire substrate.[31,36,37] Moreover, this mechanism is conducive to retention of the wire morphology, as the directed self-aggregation process of anatase TiO_2 nanocrystals has a low energy requirement for initially breaking bonds within the hydrogen titanate framework and then reforming these bonds into anatase titania.[9,37] Therefore, not surprisingly, this process can take place under moderate conditions of low temperature and low pressure, as we have observed.[37]

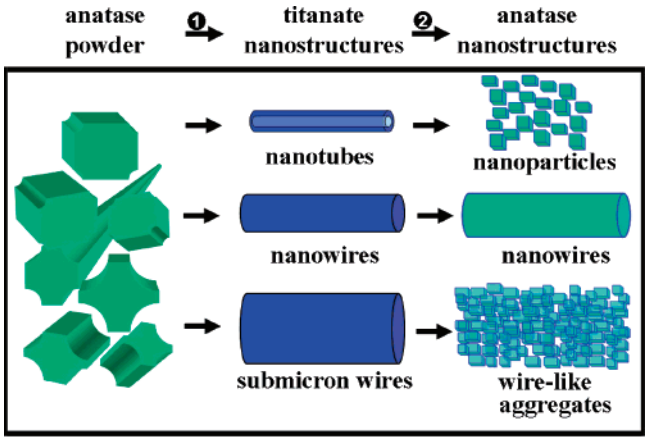

Figure 10. Schematic representation of the size- and shape-dependence of the morphological transformation of hydrogen titanate nanostructures into their anatase analogues. Step 1 represents the preparation of hydrogen titanate nanostructures, neutralized from sodium hydrogen titanate nanostructures that, in turn, had been initially hydrothermally synthesized from commercial anatase TiO_2 powder. Step 2 represents the hydrothermal size- and shape-dependent transformation process of orthorhombic protonic lepidocrocite titanate ($H_xTi_{2-x/4}\square_{x/4}O_4$ ($x \sim 0.7$, □: vacancy)) nanostructures into anatase titania nanostructures at 170 °C for 24 h.

Even so, for small precursor protonic lepidocrocite titanate nanowires (≤200 nm in diameter), it is relatively easier, based on relative growth rates along different planes, to form small equidimensional particles similar in dimension to the starting material. Therefore, for these small hydrogen titanate nanowires, their transformation to anatase TiO_2 nanowires was effectively a simple, in situ phase conversion process. Alternatively, anatase TiO_2 nanowire formation can be explained as resulting from as-formed smaller anatase TiO_2 nanoparticles more easily attaching to the hydrogen titanate nanowire surface by attractive van der Waals forces (the "hit-and-stick" scenario), subsequently aggregating, and ultimately fusing to form elongate single crystals.[38]

On the basis of the detailed analysis of the HRTEM and SAED data, the proposed size-dependent shape transformation of hydrogen titanate nanostructure precursors into their anatase TiO_2 counterparts is illustrated in Figure 10. It is expected that synthetic advances in achieving monodispersity and diameter control over the size and shape distribution of hydrogen titanate nanostructure precursors can aid in optimizing the morphological transformation process described herein.

Photocatalytic Activity. The photocatalytic activity of our as-prepared anatase TiO_2 nanostructures was evaluated by measuring the degradation of synthetic Procion Red MX-5B dye at 538 nm upon photoexcitation with light at 365 nm. It is evident that both anatase TiO_2 nanoparticles and nanowires (Figures 6 and 7, respectively), prepared from nanoscale titanate precursors, are active photocatalysts, as illustrated in Figure 11. Moreover, our as-prepared anatase TiO_2 nanoparticles (Figure 11c) and wires (Figure 11d) exhibit higher photoactivities as compared with similarly sized commercial TiO_2 nanoscale powders (Figure 11b), from whence the parent titanate nano-

(32) Yeadon, M.; Ghaly, M.; Yang, J. C.; Averback, R. S.; Gibson, J. M. *Appl. Phys. Lett.* **1998**, *73*, 3208.
(33) Penn, R. L.; Banfield, J. F. *Science* **1998**, *281*, 969.
(34) Penn, R. L.; Banfield, J. F. *Geochim. Cosmochim. Acta* **1999**, *63*, 1549.
(35) Barnard, A. S.; Curtiss, L. A. *Nano Lett.* **2005**, *5*, 1261.
(36) Banfield, J. F.; Welch, S. A.; Zhang, H.; Ebert, T. T.; Penn, R. L. *Science* **2000**, *289*, 751.
(37) Liu, B.; Yu, S.-H.; Li, L.; Zhang, F.; Zhang, Q.; Yoshimura, M.; Shen, P. *J. Phys. Chem. B* **2004**, *108*, 2788.
(38) Pei, L.; Mori, K.; Adachi, M. *Langmuir* **2004**, *20*, 7837.

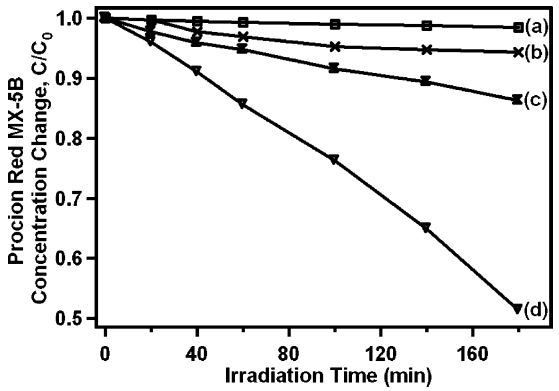

Figure 11. Photocatalytic activity of the samples in the presence of Procion Red MX-5B: (a) blank control; (b) commercial anatase TiO_2 (Alfa Aesar, 32 nm powder); (c) as-prepared anatase TiO_2 nanoparticles; (d) as-prepared anatase TiO_2 wires.

structure precursors, used to generate our titania nanostructures, were initially derived.

The observed enhancement of photocatalytic activity, relative to a commercial sample, may be related to an increase in surface area as well as with a rise in anatase mass fraction and crystallinity,[39] characteristic of our pure, as-prepared anatase titania nanostructures. Moreover, an increased amount of hydroxyl species on the surfaces of as-prepared anatase TiO_2 nanoscale samples could also explain the heightened decomposition rate observed.[25,26] In addition, it was also found that our parent titanate precursor nanostructures exhibited minimal or no catalytic performance, consistent with a previous report for undoped trititanate nanotube samples,[40a] which may be attributed to the higher band gap energy of our titanate samples relative to that of titania (Figure 3a and 3b) and hence a higher energy of irradiation (than the 365 nm light used in this study) needed for optimal photocatalytic activation. Furthermore, the anatase TiO_2 nanowires (Figure 11d) exhibited an increased photoactivity relative to that of anatase TiO_2 nanoparticles (Figure 11c). The morphology-driven energy shift and broadening of the absorption spectrum of anatase TiO_2 nanowires (Figure 3d), with respect to that of anatase TiO_2 nanoparticles (Figure 3c), can account for the increased photoactivity.[40b] As implied previously, the particulate size, degree of aggregation, surface chemistry, and surface area of these nanostructures are also important parameters that affect our data.

(39) (a) Xu, Y.; Langford, C. H. *Langmuir* **2001**, *17*, 897. (b) Jang, H. D.; Kim, S.-K.; Kim, S.-J. *J. Nanopart. Res.* **2001**, *3*, 141.

(40) (a) Hados, M.; Horvath, E.; Haspel, H.; Kukovecz, A.; Konya, Z.; Kiricsi, I. *Chem. Phys. Lett.* **2004**, *399*, 512. (b) Burda, C.; Lou, Y.; Chen, Y.; Samia, A. C. S.; Stout, J.; Gole, J. L. *Nano Lett.* **2003**, *3*, 1049.

Conclusions

In summary, we have demonstrated that a controllable size- and shape-dependent morphological change between protonic lepidocrocite titanate and anatase TiO_2 nanostructures can readily occur under relatively simple hydrothermal reaction conditions, in neutral solution, and at reasonably low temperatures. That is, the size and morphology of the nanosized reactants can dictate that of the corresponding nanosized products, an idea which has implications for nanoscale design as well as for the probing of morphology-dependent properties in nanomaterials. Moreover, the TiO_2 nanoparticulate products we have isolated are single-crystalline, of the anatase phase, and of satisfactory purity, without impurities arising from brookite or rutile, all of which are desirable characteristics for nanoparticles with potential applications in photocatalysis and other chemical processes.

Acknowledgment. Research (including facilities and personnel) was supported in part by the U.S. Department of Energy Office of Basic Energy Sciences under Contract DE-AC02-98CH10886. Acknowledgment is also made to the National Science Foundation for a CAREER award (DMR-0348239) and the donors of the Petroleum Research Fund, administered by the American Chemical Society, for PI support of this research. Y.M. recognizes Sigma Xi for a Grant-in-Aid of Research. We also thank Professor J. Huang and S. Chen at Boston College as well as Dr. J. Quinn at SUNY at Stony Brook for their help with HRTEM and SEM analyses, respectively. We appreciate the assistance of T. Hemraj-Benny at SUNY Stony Brook and Dr. Z. Nikolov at Drexel University with the Raman analyses.

Supporting Information Available: Histogram of titanate nanowires; enlarged HRTEM images and SAED pattern, associated with Figures 8 of the main text; ICP-MS data of titanate and anatase titania nanowires. This material is available free of charge via the Internet at http://pubs.acs.org.

JA0607483